Tailoring the Porous Hierarchy of Titanium Phosphates

ARTICLE *in* LANGMUIR · MAY 2006

Impact Factor: 4.46 · DOI: 10.1021/la0533011 · Source: PubMed

Tailoring the Porous Hierarchy of Titanium Phosphates

Tie-Zhen Ren,[§] Zhong-Yong Yuan,[§,†] Ammar Azioune,[#] Jean-Jacques Pireaux,[#] and Bao-Lian Su*[,§]

Laboratoire de Chimie des Matériaux Inorganiques and Laboratoire Interdisciplinaire de Spectroscopie Electronique, The University of Namur (FUNDP), 61 rue de Bruxelles, B-5000 Namur, Belgium, and Department of Materials Chemistry, Nankai University, Tianjin 300071, P.R. China

Received December 6, 2005. In Final Form: February 15, 2006

First hierarchical titanium phosphate (TiPO) materials with multiple porosities of different lengths (meso-macroporous and meso-macro-macroporous) were synthesized by the self-formation process. The further tuning of the porous hierarchy by using the poly(ethylene oxide) surfactant technique was demonstrated. The macroporous structure (50−160 nm in size) of TiPO with mesoporous walls could be self-formed in the absence of any templatable agents, including surfactant molecules. On the basis of spontaneous structurization, the addition of a small quantity of nonionic poly(ethylene oxide) surfactant (e.g., 5%) led to an improvement in macroporosity in abundance and in regularity with a slight enlargement in macropore sizes to 80−250 nm. Interestingly, a secondary, larger macropore system with parallel channels 500−1000 nm in size was generated when the synthesis was performed with moderately increasing the content of surfactant (10%), giving rise to an unprecedented trimodal meso-macro-macroporous structure. A uniform three-dimensional co-continuous macroporous structure with accessible wormhole-like mesoporous walls was synthesized by using the higher content of surfactants. This is a direct demonstration of tailoring the porous hierarchy of different lengths integrated in one solid body by fine-tuning the self-formation process and the participation of surfactant. The synthesized hierarchical titanium phosphates possess interesting optical and acidic properties, which should be significant for large application potential from catalysis and separation to electrochromic devices, fuel cells, and bioactive materials.

Introduction

Metal phosphates, such as Zr and Ti phosphates, are active solid catalysts that can be used in acid−base catalysis, redox catalysis, and photocatalytic processes.[1−3] These materials can be considered inorganic superacid solids, and are responsible for much of the catalytic activity so far observed in the literature, justified by their acidic nature, which is attributed to the Brønsted acidity of the hydroxyl groups in the interlayers and to the Lewis acidity of the metal center.[4] Their electric behavior has also been widely studied.[5] Besides the previously reported layered[4] and zeolite-like microporous[6] titanium phosphates, several mesoporous titanium phosphate (TiPO) materials have recently been synthesized by the use of cationic[7] or anionic[8] surfactants, alkylamines,[9] or block copolymers[10] as the templates. An interesting anion and cation exchange capacity of titanium phosphate was demonstrated.[8] However, there are no reports on the hierarchical porous TiPO possessing a uniform bimodal or multimodal pore structure to date.

Practical approaches do require the preparation of mesoporous materials having hierarchical porous structures at different length scales in order to achieve highly organized functions.[11] This is partly because hierarchical materials with different pore sizes integrated in one body can be expected to combine reduced resistance to diffusion and high surface areas to yield improved overall reaction and adsorption/separation performances and can be extended to biological applications. Fluid catalytic cracking (FCC) catalysts are concrete examples of hierarchical structures used in industry and involve the formation of a composite principally from a main component, an ultrastable Y (USY) zeolite mixed with a macroporous matrix, usually amorphous silica, alumina, or silica/alumina with clay. The dealumination treatment by water vapor steaming at 400−500 °C or a chemical solution of $(NH_4)_2SiF_6$ can bring a poorly defined mesoporosity due to the removal of Al atoms from the zeolite framework. The precracking of the heavy feedstocks prior to the action of the USY zeolite is carried out in the macroporous matrix. The microporous openings of zeolites, however, impede the diffusion of bulky molecules from vacuum gas−oil and residues. Thus, the presence of mesoporosity in USY zeolites facilitates the secondary catalytic cracking. Finally, the more oriented cracking and the fine rearrangement of cracked molecules take place in the supercages of USY zeolites. However, this micro-meso-macroporous hierarchy was obtained by the artificial mixture of different components containing predefined porosities.

Although the combination of the surfactant templating techniques and the micromold methods of emulsion droplets,[12,13]

* To whom correspondence should be addressed. Fax: +32-81-725414. Tel: +32-81-724531. E-mail: bao-lian.su@fundp.ac.be.

[§] Laboratoire de Chimie des Matériaux Inorganiques.

[#] Laboratoire Interdisciplinaire de Spectroscopie Electronique.

[†] Nankai University.

(1) La Ginestra, A.; Patrono, P.; Berardelli, M. L.; Galli, P.; Ferragina, C.; Massucci, M. A. *J. Catal.* **1987**, *103*, 346−356.

(2) Frianeza, T. N.; Clearfield, A. *J. Catal.* **1984**, *85*, 398−404.

(3) Rocha, G. M. S. R. O.; Johnstone, R. A. W.; Neves, M. G. P. M. S. *J. Mol. Catal. A* **2002**, *187*, 95−104.

(4) Clearfield, A.; Costantino, U. In *Comprehensive Supramolecular Chemistry*; Alberti, G., Bein, T., Eds.; Elsevier: Amsterdam, 1996; Vol. 7, pp 107−150.

(5) Alberti, G.; Casciola, M. In *Proton Conductors*; Colomban, P., Ed.; Cambridge University Press: Cambridge, UK, 1992; pp 238−251.

(6) Ekambaram, S.; Sevov, S. C. *Angew. Chem., Int. Ed. Engl.* **1999**, *38*, 372−375.

(7) Jones, D. J.; Aptel, G.; Brandhorst, M.; Jacquin, M.; Roziére, J.; Jiménez-Jiménez, J.; Jiménez-López, A.; Maireles-Torres, P.; Piwonski, I.; Rodríguez-Castellón, E.; Zajac, J.; Rozière, J. *J. Mater. Chem.* **2000**, *10*, 1957−1963.

(8) Bhaumik, A.; Inagaki, S. *J. Am. Chem. Soc.* **2001**, *123*, 691−696.

(9) Pan, C. L.; Zhang, W. X.; Wang, Y. L.; Zhou, Z.; Jiang, D. Z.; Wu, S. J.; Wu, T. H. *Mater. Lett.* **2003**, *57*, 3815−3819.

(10) Tian, B.; Liu, X.; Tu, B.; Yu, C.; Fan, J.; Wang, L.; Xie, S.; Stucky, G. D.; Zhao, D. *Nat. Mater.* **2003**, *2*, 159−163.

(11) Maekawa, H.; Esquena, J.; Bishop, S.; Solans, C.; Chmelka, B. F. *Adv. Mater.* **2003**, *15*, 591−596.

(12) Antonelli, D. M. *Microporous Mesoporous Mater.* **1999**, *33*, 209−214.

(13) Yuan, Z. Y.; Ren, T. Z.; Su, B. L. *Adv. Mater.* **2003**, *15*, 1462−1465.

10.1021/la0533011 CCC: $33.50
Published on Web 03/15/2006

colloid crystals,[14,15] or bacterial threads[16] could allow the construction of hierarchically mesoporous−macroporous oxide materials, the design and preparation of high-surface-area materials with multiscaled porous structures is still an experimental challenge. Hierarchical bimodal mesoporous−macroporous metal oxides have been synthesized in the presence of a single surfactant,[17−21] without the need of polymeric spheres or vesicles to act as a template that generates the macroporous structure, having channel-like macropores of one-dimensional orderliness that are distinct from those templated by latex spheres or vesicles or formed by polymerization-induced phase separation.[22] Suzuki et al.[23] synthesized mesoporous silica foams with a hierarchical trimodal pore structure (macrovoids and two kinds of mesopores ranging between 3 and 40 nm) by the self-assembly of surfactant micelles, silica nanoparticles and air bubbles. Smått et al.[24] utilized poly(ethylene glycol) and alkylammonium surfactants together, which they called "double-templating synthesis", for the preparation of silica monoliths exhibiting a trimodal pore structure where macropores resulted in phase separation and gelation kinetics, textural mesopores of 10−20 nm size originated from voids between particles, and internal mesopores of 2−4 nm in the particles were from supramolecular templating of the surfactant. The phase-separation-induced formation of macro-mesoporous ethane−silica gels has also recently been reported with the aid of a block copolymer.[25] A surfactant and/or polymer were believed to be necessary in the formation of these hierarchical oxide materials.[17−22,24,25]

Very recently, the spontaneous template-free assembly of ordered macroporous titania, aluminosilicate, and other metal oxides was reported.[26−30] Thermally stable macroporous zirconium phosphates with supermicroporous walls were also produced in the absence of organic templates,[27] indicating a self-formation phenomenon of hierarchy. Thus, it seems the surfactants or polymers may not necessarily be directly involved in the formation of hierarchical porous structures. Do the surfactants or polymers take a role in the hierarchy formation, even in the mesopore formation of a macroporous framework? The answer would seem to be drawn from a very recent and very comprehensive paper on the formation of hierarchically structured pure aluminas made by Shanks and Deng.[28] They demonstrated that the mesoporous structure, which was created by the interstitial porosity between boehmite nanoparticles, was formed independently of the macropores and was not significantly impacted by the use of a surfactant, whereas the formation of the macropores required the presence of an alkoxide droplet within the synthesis mixture, and the surfactant played no role other than to influence the hydrodynamic conditions during synthesis. The control of the hydrodynamic conditions is crucial and a key factor in the formation of a macroporous structure, as claimed by Mann et al. on the basis of their experience in the spontaneous synthesis of macroporous titania.[26] Because of the divergent observations and despite a large series of works realized in different groups,[17−21,26−32] the real and precise formation mechanism of these hierarchical meso-macroporous structures with the help of alkoxides remains elusive.[28] Until now, neither the spontaneous process nor the soft templating method reported in the literature allowed control of the macrochannel size, and the hierarchical structure could be only formed under limited mixing conditions.[28] Following our previous and actual works[13,17−20,27,29,32] and those published by Mann et al.[26] and Shanks et al.,[21,28] we describe herein the hierarchical TiPO materials with uniform multiple-scaled porosity. The formation of well-defined small macropore (50−160 nm in size) systems with mesoporous walls could be spontaneously acquired in the absence of any surfactant molecules and/or templates (such as colloid crystals and emulsion droplets), while the third tier of large macropores (500−1000 nm in size), in the form of parallel channels, could be originated from the participation of the PEO−surfactant molecules. This is the first example of hierarchical mesoporous materials with a well-defined bimodal macroporous structure. This is also the first illustration of how the different pore-size lengths can be integrated in one solid compound by adjusting the self-formation process and the assistance of the surfactant molecules. This study could be of importance and can shed some light on the rational design of the hierarchically porous materials with different pore size by the combination of a spontaneous formation process and the assistance of surfactant molecules or other templating agents. Furthermore, the synthesized hierarchical TiPO materials possess acidic and optical properties, which suggest their practical application potential.

Experimental Section

Synthesis. All chemicals were used as received without further purification. In a typical synthesis procedure, 0.01 mol of titanium tetrapropoxide ($Ti(OC_3H_7)_4$, 98% solution, Merck) was added into a pretreated 60 mL solution of orthophosphoric acid (0.1 mol/L). To tailor the porous hierarchy to different pore size lengths, different contents of surfactant Brij 56 ($C_{16}(EO)_{10}$, Aldrich) were introduced to the orthophosphoric acid solution and homogenized prior to the addition of the titanium precursor under stirring. After stirring for an additional 2 h at room temperature, the obtained mixture was sealed in one Teflon-lined autoclave and aged statically at 80 °C for 24 h. The product was filtered, washed with water, and dried at 60 °C (denoted as TiP−S*x* or TiP−N for the sample synthesized with or without surfactant, respectively, where *x* refers to the content of the surfactant, such as 5, 10, or 15 wt %). The TiP−S*x* samples were Soxhlet-extracted with ethanol solution for 36 h to remove the surfactant species. To investigate the thermal stability, the as-synthesized TiPO samples were calcined at 300 and 550 °C for 2 h.

Characterization. Powder X-ray diffraction (XRD) patterns were recorded on a Philips PW1820 diffractometer with Cu Kα radiation. N_2 adsorption and desorption isotherms were obtained on a Micromeritics Tristar 3000 system at liquid nitrogen temperature. The samples were degassed at 80 °C overnight before measurements were made. The specific surface area was determined by the

(14) Holland, B. T.; Blanford, C. F.; Do, T.; Stein, A. *Chem. Mater.* **1999**, *11*, 795−805.
(15) Davis, S. A.; Burkett, S. I.; Mendelson, N. H.; Mann, S. *Nature* **1997**, *385*, 420−423.
(16) Lebeau, B.; Fowler, C. E.; Mann, S.; Farcet, C.; Charleux, B.; Sanchez, C. *J. Mater. Chem.* **2000**, *10*, 2105−2108.
(17) Blin, J. L.; Léonard, A.; Yuan, Z. Y.; Gigot, L.; Vantomme, A.; Cheetham, A. K.; Su, B. L. *Angew. Chem. Int. Ed.* **2003**, *42*, 2872−2875.
(18) Ren, T. Z.; Yuan, Z. Y.; Su, B. L. *Langmuir* **2004**, *20*, 1531−1534.
(19) Léonard, A.; Blin, J. L.; Su, B. L. *Chem. Commun.* **2003**, 2568−2569.
(20) Yuan, Z. Y.; Vantomme, A.; Léonard, A.; Su, B. L. *Chem. Commun.* **2003**, 1558−1559.
(21) Deng, W.; Toepke, M. W.; Shanks, B. H. *Adv. Funct. Mater.* **2003**, *13*, 61−65.
(22) Nakanishi, K.; Takahashi, R.; Nagakane, T.; Kitayama, K.; Koheiya, N.; Shikata, H.; Soga, N. *J. Sol−Gel Sci. Technol.* **2000**, *17*, 191−210.
(23) Suzuki, K.; Ikari, K.; Imai, H. *J. Mater. Chem.* **2003**, *13*, 1812−1816.
(24) Smått, J.-H.; Schunk, S.; Lindén, M. *Chem. Mater.* **2003**, *15*, 2354−2361.
(25) Nakanishi, K.; Kobayashi, Y.; Amatani, T.; Hirao, K.; Kodaira, T. *Chem. Mater.* **2004**, *16*, 3652−3658.
(26) Collins, A.; Carriazo, D.; Davis, S. A.; Mann, S. *Chem. Commun.* **2004**, 568−569.
(27) Ren, T. Z.; Yuan, Z. Y.; Su, B. L. *Chem. Commun.* **2004**, 2730−2731.
(28) Deng, W.; Shanks, B. H. *Chem. Mater.* **2005**, *17*, 3092−3100.
(29) Leonard, A.; Su, B.-L. *Chem. Commun.* **2004**, 1674−1675.
(30) Su, B.-L.; Leonard, A.; Yuan, Z.-Y. C. R. *Chimie* **2005**, *8*, 713−726.
(31) Ren, T.-Z.; Yuan, Z.-Y.; Su, B.-L. *Chem. Phys. Lett.* **2003**, *374*, 170−175.
(32) Yuan, Z.-Y.; Ren, T.-Z.; Vantomme, A.; Su, B.-L. *Chem. Mater.* **2004**, *16*, 5096−5106.

Brunauer−Emmett−Teller (BET) method, and the pore size distribution was obtained from the N_2 adsorption branch of the isotherms using the Barrett−Joyner−Halenda (BJH) method.

Scanning electron microscopy (SEM) and transmission electron microscopy (TEM) were carried out with a Philips XL-20 at 15 keV and a Philips TECNAI-10 at 100 kV, respectively. The specimens for TEM observation were prepared by epoxy-resin-imbedded microsectioning and mounting on a copper grid. Solid-state ^{31}P magic-angle spinning (MAS) nuclear magnetic resonance (NMR) spectra were recorded on a Bruker MSL-400 spectrometer operating at resonance frequencies of 161.9 MHz and a 2.5 μs ($\theta = \pi/6$) pulse with a repetition time of 10 s. Chemical shifts were indicated using an external 85% H_3PO_4 reference.

Ultraviolet−visible (UV−vis) spectra were measured in a diffuse reflectance mode on a Perkin-Elmer Lambda 35 spectrometer, with $BaSO_4$ as reference. Fourier transform infrared (FT-IR) spectroscopy was performed with a Perkin-Elmer Spectrum 2000 spectrometer. KBr pellet technique was used for the framework vibration characterization. For the characterization of the surface acidity, a self-supported wafer of TiPO sample was evacuated in situ at 450 °C for 3 h, followed by the adsorption of NH_3 at room temperature for 15 min, and desorption at different temperatures (100−200 °C) for 15 min, respectively.

X-ray photoelectron spectroscopy (XPS) measurements were performed on a Hewlett-Packard 5950A spectrometer equipped with a monochromatic Al Kα source (1486.6 eV). Charging effects were neutralized using a flood gun typically operated at 2 eV. The takeoff angle analysis relative to the surface was 45°. All the spectra showed a small shift due to charging and were therefore calibrated in relation to the C_{1s} peak of contamination (285.0 eV). The photoemission peaks were fitted with mixed Gaussian−Lorentzian functions using a home-developed least-squares curve-fitting program (Winspec) (LISE). Both linear and Shirley backgrounds were used, depending on the shape of spectra. The surface atomic composition was calculated by the integration of the peak areas on the basis of Scofield's sensitivity factors.

Results and Discussion

Synthesis and Porous Hierarchy by Electron Microscopy. Titanium tetrapropoxide was added into an orthophosphoric acid solution in the presence or absence of surfactant Brij 56 ($C_{16}(EO)_{10}$), followed by autoclaving at 80 °C for 24 h. The products synthesized with surfactant were denoted as TiP−S*x* for different surfactant contents (*x*%), and the surfactantless synthesized samples were denoted as TiP−N. The product particles of both TiP−S*x* and TiP−N are mainly tens to several tens of micrometers in size with irregular shapes, and novel porous structures can be seen in these products (Figures 1−4). SEM images show that TiP−N presents a uniform macroporous structure with pore sizes in the range of 50−160 nm (Figure 1a). This macroporous structure is further confirmed by the cross-sectional low magnification TEM images (Figure 1b). Moreover, the high-magnification TEM images clearly reveal that the walls of a macroporous network of TiP−N are composed of accessible mesopores with a wormhole-like array (Figure 1c). Such unusual hierarchical structures can be retained after calcination at 550 °C, showing high thermal stability. The genesis of this meso-macroporous hierarchy in the absence of the surfactant molecules corresponds to a spontaneous formation mechanism, as described by Mann et al.[26] and in our previous work.[27,29] The present hierarchical meso-macroporous titanium phosphate is being reported for the first time.

When a 5 wt % surfactant solution was introduced into the synthesis gel, the resultant product, TiP−S5, exhibited a very high macroporosity, contrary to TiP−N (Figure 2), in which the average macropore size increases from 50−160 to 80−250 nm. This implies that the use of a small content of surfactant molecules could modify the macroporosity of the resultant TiPO materials, not only in the abundance, but also in the regularity of macrochannels.

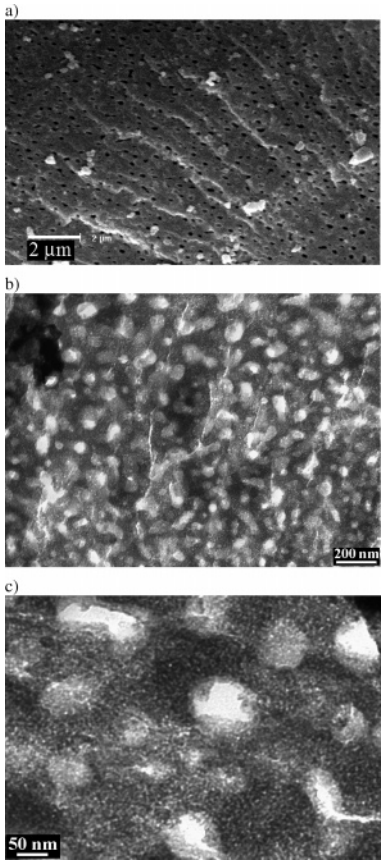

Figure 1. (a) Representative SEM and (b,c) cross-sectional TEM images of the surfactantless synthesized TiP−N sample.

Interestingly, with the increase in the surfactant content of the reaction system to 10 wt %, the resultant TiP−S10 sample presents the generation of a secondary and very large macropore array distributed among the well-defined small macropores of 80−250 nm (Figure 3a). The secondary and very large macropores are channel-like, parallel to each other (Figure 3b), and 500−1000 nm in size of homogeneous distribution, which is quite similar to those of previously reported surfactant-assisted meso-macrostructured metal oxide materials.[17−21] The small macropores are distributed in the walls separating the large macropores, forming a hierarchical structure, which is confirmed by cross-sectional TEM images (Figure 3b,c). And the walls between these macropores are mesostructured with wormhole-like assembly (Figure 3d). A hierarchy with three different pore-size lengths (mesopores, small macropores, and large macropores) is integrated into one solid body of titanium phosphate. These kinds of materials could be of great importance in the design of structured catalysts for one-pot reactor processes.

The further increase of the surfactant content to 15 wt % results in an alternative macroporous structure. Figure 4 shows the SEM and TEM images of the TiP−S15 sample, representing well-defined co-continuous macropores with the pore diameters around 500−1500 nm. The macroporous walls are also composed of accessible mesopores with a wormhole-like array.

Phase Identification and Textual Characteristics by XRD and N_2 Adsorption Analysis. All the synthesized TiPO samples possess amorphous framework walls, as revealed by powder XRD patterns (Figure 5). No crystallized TiP_2O_7 or TiO_2 phases appear, even after calcination at 550 °C. There are no low-angle

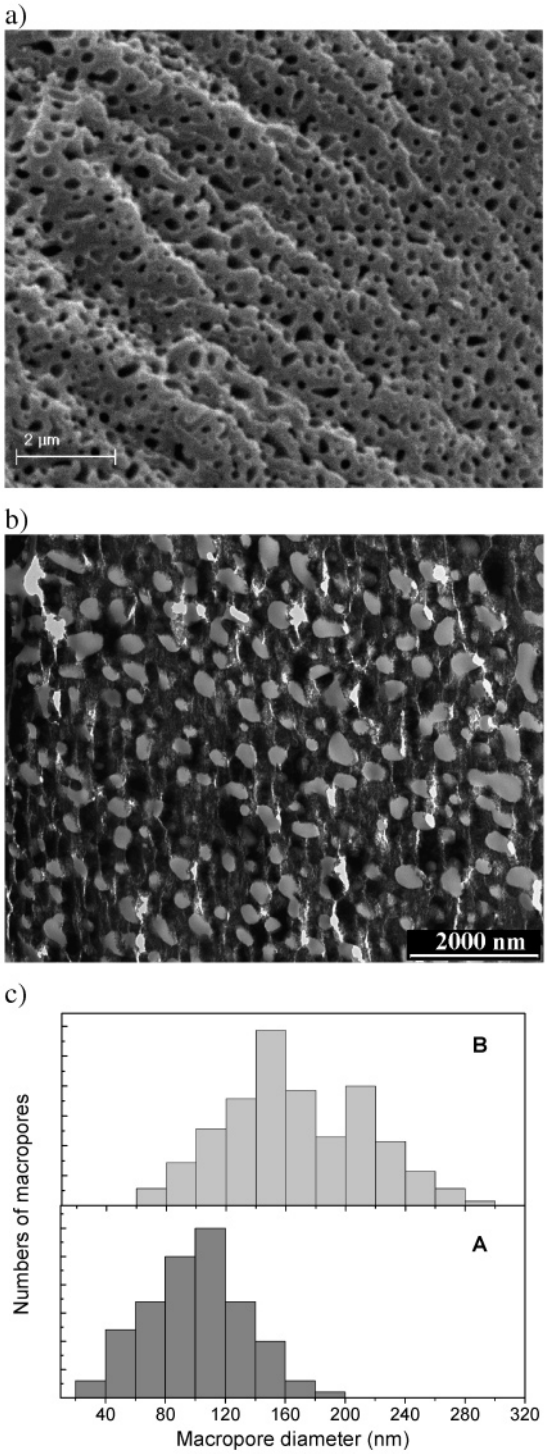

Figure 2. (a) SEM and (b) cross-sectional TEM images of the TiP−S5 sample synthesized with a 5% content of surfactant. (c) Plots of macropore size distributions of the (A) TiP−N and (B) TiP−S5 samples using the measurements from more than 500 macropores

.

diffraction peaks observed in the 2θ range from 1.0 to 3.0° for the samples synthesized in the absence of surfactant or with a low content of surfactant (TiP−N and TiP−S5), while one very broad diffraction line could be visible in the low-angle diffraction patterns of the samples synthesized with a very high content of surfactant (e.g., TiP−S15). This indicates the nonexistence of a long-range order of mesopore arrays in these hierarchical TiPO materials.

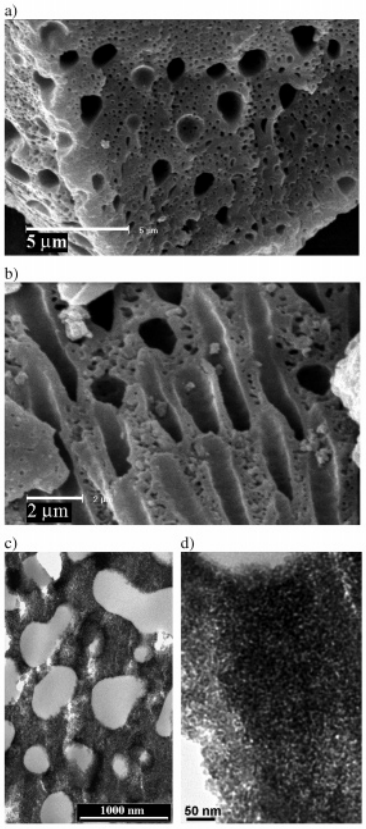

Figure 3. (a,b) Representative SEM images of the hierarchical TiP−S10 sample synthesized with a 10% content of surfactant, viewed from different directions, and (c,d) cross-sectional TEM images at different magnifications.

Figures 6 and 7 show the N_2 adsorption−desorption isotherms and the corresponding pore size distribution curves of the synthesized samples TiP−N and TiP−S10, respectively. All isotherms are of type IV and characteristic of mesoporous materials. However, those of the TiP−S10 samples (Figure 7) become more or less sloping, indicating that the surfactant present in the synthesis system can affect the mesoporous texture. The pore size distribution is obtained from an analysis of the adsorption branch of the isotherms by the BJH method. The pore sizes of the as-prepared TiP−N and TiP−S10 are centered at 2.5 nm. Although the surface area and pore volume of the as-prepared TiP−N (304 m^2/g and 0.346 cm^3/g, respectively) are larger than those of the as-prepared TiP−S10 (228 m^2/g and 0.284 cm^3/g, respectively), the surface area and pore volume of TiP−S10 after extraction (312 m^2/g and 0.367 cm^3/g, respectively) become highest, indicating that the surfactant species existed in the as-prepared TiP−S material and could be removed by ethanol extraction. Their surface areas and pore volumes decrease after calcination, while the pore sizes increase with the calcination temperature, suggesting a nanoparticle assembly mechanism for the formation of mesoporous frameworks. In fact, because of the increased crystallization during the calcinations, the growth of nanoparticles occurs, and the interspaces between the particles will be enlarged, leading to the enlargement of the mesopore size.[18,28,31] The global textural properties of the uncalcined and calcined TiP−N and TiP−S10 samples are listed in Table 1. It is seen that the surface area and pore volume of TiP−S10 decrease less rapidly than those of TiP−N, suggesting that the surfactant-assisted TiP−S*x* has higher thermal stability than the surfactantless synthesized TiP−N. The mesoporosities revealed by the traditional N_2-adsorption method are in agreement with the wormhole-

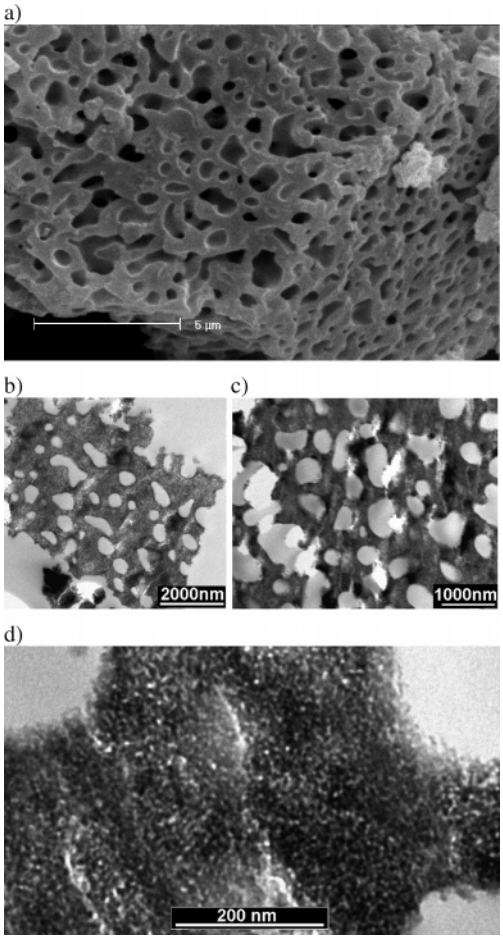

Figure 4. (a) Representative SEM image of the hierarchical TiP−S15 sample synthesized with a 15% content of surfactant, and (b−d) cross-sectional TEM images at different magnifications.

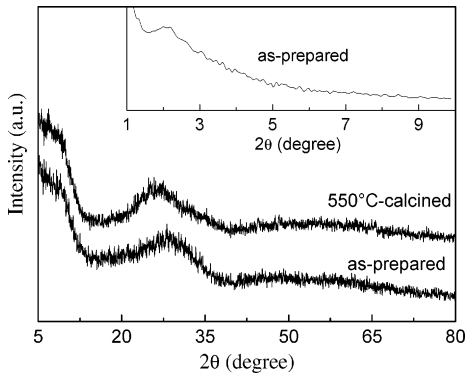

Figure 5. XRD patterns of the as-synthesized and 550-°C-calcined TiP−S15 samples. Inset is the low-angle diffraction pattern of the as-synthesized form.

like mesostructures in the macroporous frameworks of the synthesized TiPO materials observed by high-magnification TEM images.

Chemical Composition, Skeletal Structure, and Chemical Environment by XPS, FT-IR, and Solid-State NMR. Figure 8 shows the high-resolution XPS spectra of Ti and P taken on the surface of as-synthesized and 550-°C-calcined TiP−S10 samples. Other TiP−S*x* and TiP−N samples exhibit the same spectra. The Ti2p line is composed of two single peaks situated at 459 eV for $Ti2p_{3/2}$ and 464.8 eV for $Ti2p_{1/2}$. These binding energies are characteristic of Ti^{4+}.[33,34] The P2p binding energy is observed at 133.6 ± 2 eV for both the as-synthesized and

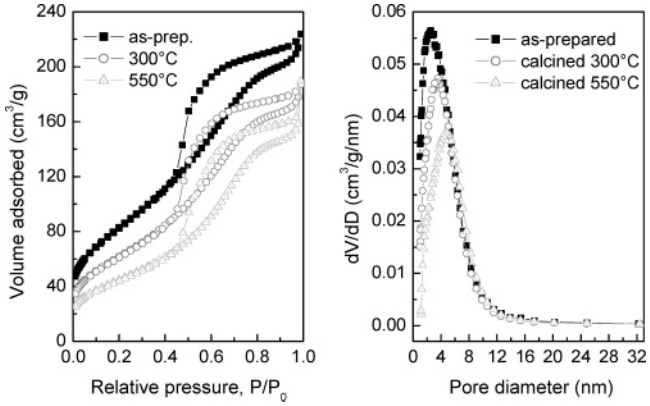

Figure 6. N_2 adsorption−desorption isotherms (left) and the corresponding BJH pore size distribution curves (right) of the as-prepared and calcined TiP−N samples.

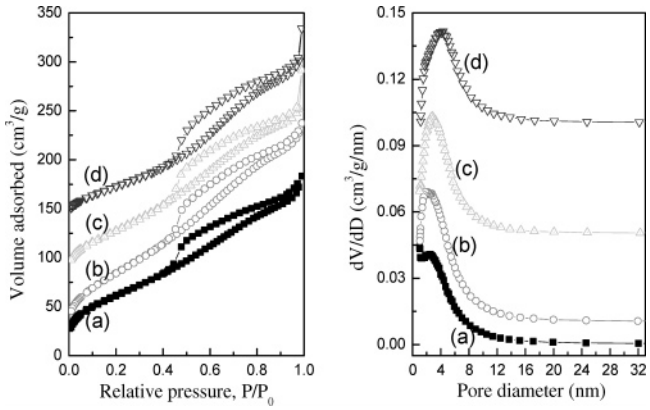

Figure 7. N_2 adsorption−desorption isotherms (left) and the corresponding BJH pore size distribution curves (right) of the TiP−S10 samples: (a) as-synthesized; (b) extracted; (c) 300-°C-calcined; (d) 550-°C-calcined. The volume adsorbed was shifted by 0, 60, and 120, and the d*V*/d*D* value was shift by 0.01, 0.05, and 0.10 for the curves of b, c, and d, respectively.

calcined TiPO materials, which is characteristic of P^{5+}.[35] Since the P2p peaks appear at a high binding energy, and no peaks appear at 128.6 eV, which is the characteristic binding energy of P in TiP,[36] there is no possibility for the presence of Ti−P bonds in our hierarchical TiPO materials.

Figure 9 shows the high-resolution XPS spectra of the oxygen O1s region of the TiPO before and after calcination at 550 °C. The broad peak of O1s might be fitted by four components, situated at 530.2, 531.2, 532.2, and 533.4 eV (error ± 0.3 eV). These binding energies can be assigned to O−Ti, O−P, O−H, and O−C bonds, respectively,[37] and their proportions in contribution are also listed in Table 1. The O1s component of the O−P bonds is dominant, which contributes a proportion exceeding 45% in all the materials (Table 1). The component characteristic of the O−Ti bonds increases after calcination, and the components of the hydroxyl groups and O−C bonds decrease. This indicates that the decomposition of surface water and removal of organic species during the calcination accompanies the strengthening of Ti−O−P network.

(33) Briggs, D., Seah, M. P., Eds. *Practical Surface Analysis*, 2nd ed.; Auger and X-ray Photoelectron Spectroscopy; Wiley: New York, 1999; Vol. 1.
(34) Pétigny, S.; Mostéfa-Sba, H.; Domenichini, B.; Lesniewska, E.; Steinbrunn, A.; Bourgeois, S. *Surf. Sci.* **1998**, *410*, 250−257.
(35) Splinter, S. J.; Rofagha, R.; Mcintyre, N. S.; Erb, U. *Surf. Interface Anal.* **1996**, *24*, 81.
(36) Baunack, S.; Oswald, S.; Scharnweber, D. *Surf. Interface Anal.* **1998**, *26*, 471−479.
(37) Yu, J. C.; Zhang, L.; Zheng, Z.; Zhao, J. *Chem. Mater.* **2003**, *15*, 2280−2286.

Table 1. Textural Properties of the Synthesized TiPO Materials and Their Surface Atomic Compositions Obtained by XPS Analysis

sample	processing	S_{BET} (m^2/g)	D_{BJH} (nm)	V_{pore} (cm^3/g)	Ti/P ratio	O/P ratio	O_{1s} component (%)			
							O−Ti	O−P	O−H	O−C
TiP−S10	as-prepared	228	2.5	0.284	1	5	21.7	44.0	28.9	5.4
	extracted	312	2.2	0.367	1	5				
	300-°C-calcined	250	2.8	0.358						
	550-°C-calcined	195	4.1	0.331	1.1	5.3	32.7	52.9	8.6	5.8
TiP−N	as-prepared	304	2.5	0.346	1	5.5	21.1	50.5	18.0	10.4
	300-°C-calcined	227	3.6	0.289						
	550-°C-calcined	165	4.8	0.293	1.1	5.5	32.2	46.0	9.9	11.9

The surface atomic composition of the materials was calculated, and it is found that the Ti/P atomic ratio is 1 in the as-synthesized form and 1.1 in the calcined product (Table 1), whether the material was prepared with or without surfactant. The Ti/P ratios confirm the exclusive formation of $Ti(PO)_x$ (Ti polyphosphate or phosphated titania). The O/P ratios are relatively higher than the theoretical values, which should be equal to 4 (Table 1). The excess of the oxygen may be from the surface absorbed water and the organic contaminant confirmed by the XPS spectra of the C1s region.

The FT-IR spectra of as-synthesized and 550-°C-calcined TiPOs (the TiP−S10 sample being taken as representative) are shown in Figure 10. The spectrum of the as-synthesized sample exhibits absorption bands in the region of 2850−2920 cm^{-1}, attributed to the C−H stretching mode of hydrocarbons, and the band at 1460 cm^{-1}, assigned to the bending vibration of the C−H band of methylene groups of the surfactant alkyl chain, which disappear after calcination. The broad band at 3400 and the band at 1630 cm^{-1} correspond to the surface-adsorbed water and hydroxyl groups,[31] whose intensities decrease after calcination. The band at 1000−1050 cm^{-1} could be attributed to the Ti−O−P framework vibrations,[8] which is absent in the mesoporous TiO_2, suggesting a Ti−O−P network in the hierarchical TiPO materials. The small band at 1400 cm^{-1} due to the presence of the phosphoryl (P═O) frequency of PO_4^{3-}, and very weak bands around 760 cm^{-1} corresponding to P−O−P deformation vibrations[38] are also observed in the IR spectra of both the as-synthesized and calcined samples. This implies that is very

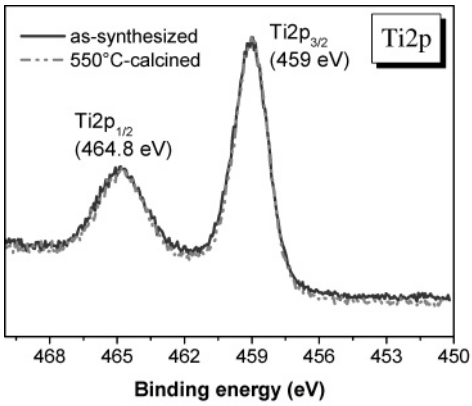

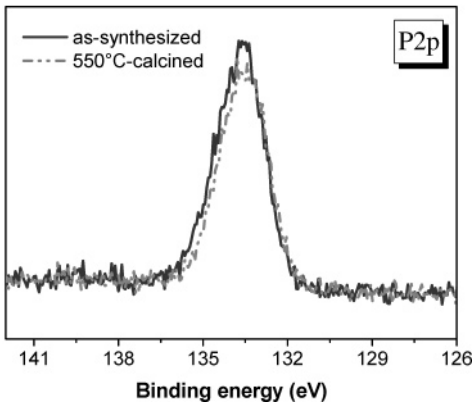

Figure 8. High-resolution XPS spectra of the Ti2p and P2p regions taken on the surface of the as-synthesized and 550-°C-calcined TiP−S10 samples.

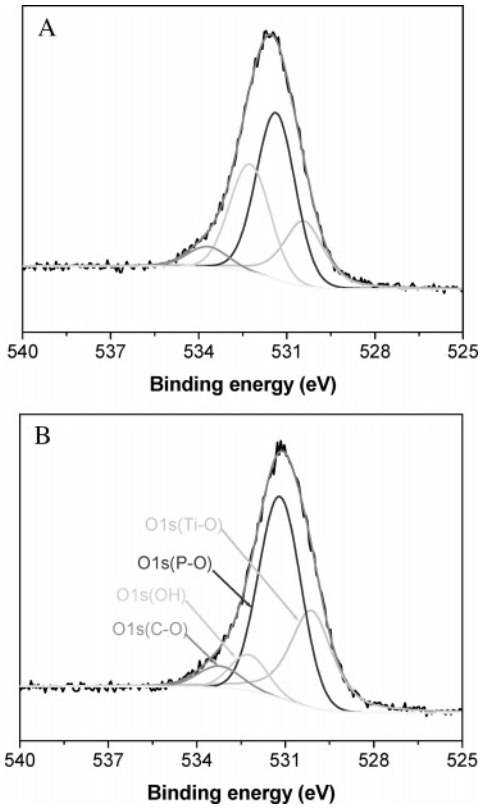

Figure 9. High-resolution XPS spectra of the O1s region taken on the surface of the (A) as-synthesized and (B) 550-°C-calcined TiP−S10 samples.

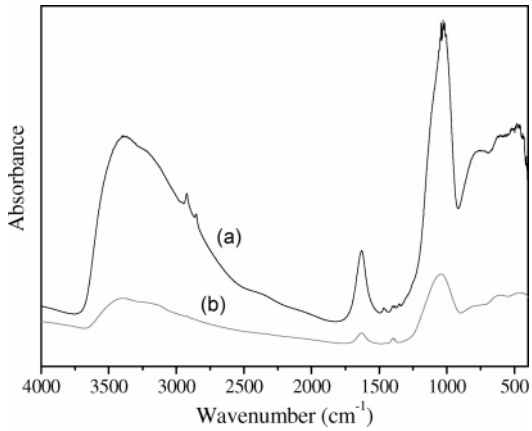

Figure 10. Skeletal FT-IR spectra of the (a) as-synthesized and (b) 550-°C-calcined TiP−S10 samples.

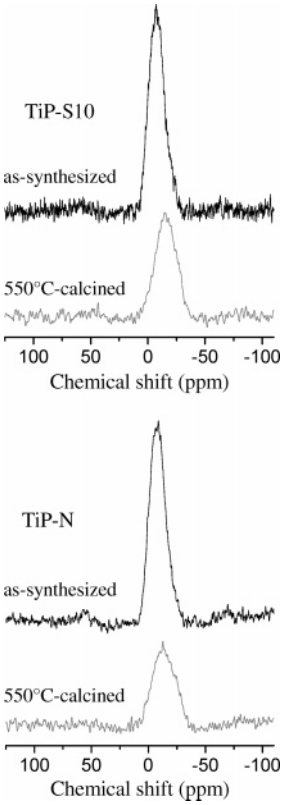

Figure 11. ^{31}P MAS NMR spectra of the as-synthesized and calcined TiPO materials.

probable that some unconsumed orthophosphoric acid molecules remain impregnated on the TiPO solids, confirming the conclusion from XPS.

^{31}P MAS NMR spectroscopy was employed to study the phosphorus microenvironments. The as-prepared TiP−S10 gives one intense peak at a chemical shift of −7 ppm, and 550-°C-calcined TiP−S10 shows one peak at −16 ppm with reduced intensity (Figure 11). The ^{31}P MAS NMR spectra of as-prepared and 550-°C-calcined TiP−N show the peaks at −8.5 and −14 ppm, respectively. The relatively broad resonance may be due to the amorphous nature of the frameworks, which lack the atomic resolution that is present in the crystalline microporous phosphates. It is believed that the chemical shifts of P atoms change toward high magnetic fields, depending on the number of metal atoms bonded to PO_4 units.[39] The peaks of −7 and −8.5 ppm in the as-prepared TiPO materials may be attributed to the PO_4 units bonded only with one or two Ti atoms through nonprotonated oxygen atoms,[39−41] that is, $P(OTi)_x(OH)_{4-x}$, where $x = 1$ or 2. The signals at −14 and −16 ppm in the 550-°C-calcined products can be assigned to tetrahedral phosphorus environments connected with three O−Ti bands [$(P(OTi)_3OH$],[34−37] indicating the possibility of modulating their acidity.[38] Further calcination at 650 °C can result in the shifts of the signals to −26 to −31 ppm, which can be attributed to the $P(OTi)_4$ species.

Optical Properties. UV−vis diffuse reflectance spectroscopy was carried out in order to find a clue to the optical properties and electronic structure of the hierarchical TiPO materials. Figure 12 shows the diffuse reflectance spectra of the as-synthesized and calcined TiPO samples, on which low reflectance means high absorption in the corresponding wavelength. The spectra of TiP−N and TiP−S*x* are almost the same. The onset wavelength of absorption (λ_{onset}) for the calcined TiPO is about 415 nm, which is larger than the reported λ_{onset} of TiO_2 (about 400 nm).[42] The band gap (E_g) of the calcined TiPO is estimated to be 2.99 eV from absorption spectra by a linear fit of the square root of the absorption coefficient ($\alpha^{1/2}$) as a function of the photon energy ($h\nu$) near the band gap.[42] This value is slightly higher than the reported E_g of TiP_2O_7 (2.95 eV),[43] but lower than the reported E_g of TiO_2 (3.0 eV for rutile and 3.2 eV for anatase).[44] The origin of the optical energy gap in the amorphous hierarchical TiPO is due to the charge-transfer excitation of electrons.

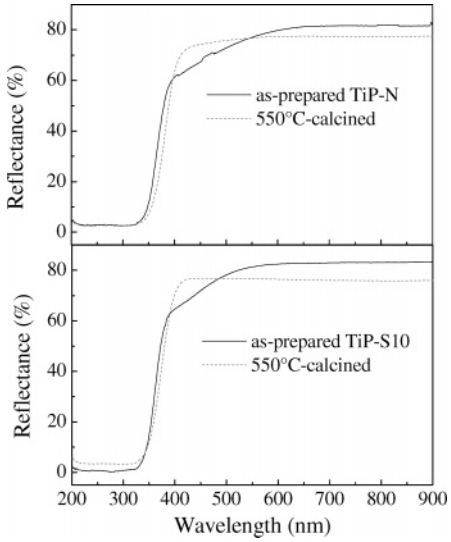

Figure 12. UV−vis diffuse reflectance spectra of the as-synthesized and calcined hierarchical TiPO samples.

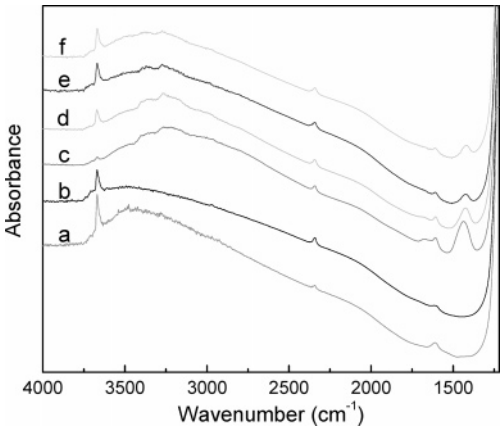

Figure 13. In situ FT-IR spectra of the calcined TiPO samples (a) after evacuation at 200 °C for 3 h, (b) after evacuation at 450 °C for 3 h, and then (c) after the adsorption of NH_3 at room temperature for 15 min, (d) after desorption at 100 °C for 15 min, (e) after desorption at 150 °C for 15 min, and (f) after desorption at 200 °C for 15 min.

Surface Acidity by Ammonia Adsorption−Desorption. Figure 13 reports the FT-IR spectra of the calcined TiPO samples in the range of 4000−1200 cm^{-1} after evacuation at 200 and 450 °C over 3 h in a vacuum line, following the adsorption and

(38) Jiménez-Jiménez, J.; Maireles-Torres, P.; Olivera-Pastor, P.; Rodríguez-Castellón, E.; Jiménez-López, A.; Jones, D. J.; Rozière, J. *Adv. Mater.* **1998**, *10*, 812−815.

(39) Wang, L.; Tian, B.; Fan, J.; Liu, X.; Yang, H.; Yu, C.; Tu, B.; Zhao, D. *Microporous Mesoporous Mater.* **2004**, *67*, 123−133.

(40) Sayari, A.; Moudrakovski, I.; Reddy, J. S. *Chem. Mater.* **1996**, *8*, 2080−2088.

(41) Schmutz, C.; Barboux, P.; Ribot, F.; Taulelle, F.; Verdaguer, M.; Fernandez-Lorenzo, C. *J. Non-Cryst. Solids* **1994**, *170*, 250−262.

(42) Du, G. H.; Chen, Q.; Han, P. D.; Yu, Y.; Peng, L.-M. *Phys. Rev. B* **2003**, *67*, 035323.

(43) Imanaka, N.; Masui, T.; Hirai, H.; Adachi, G. *Chem. Mater.* **2003**, *15*, 2289−2291.

(44) Mills, A.; Hunte, S. L. *J. Photochem. Photobiol. A* **1997**, *108*, 1−35.

desorption of ammonia molecules. One very strong band at 3670 cm^{-1} and one weak band at 1600 cm^{-1} are observed after evacuation at 200 °C (Figure 13a). The former can be assigned to the P−OH groups, indicative of the relatively weak Brønsted acid sites, and the later is attributed to the surface hydroxyl groups.[31] This also confirms the XPS results. The band at 3670 cm^{-1} is still strong after evacuation at 450 °C (Figure 13b), indicative of the existance of a large quantity of P−OH groups and a small quantity of surface hydroxyl groups in the present TiPO materials, even after such a severe evacuation. After in situ adsorption of NH_3, the intensity of the P−OH band obviously decreases, and a very broad band centered at 3250 cm^{-1} appears. This broad band is generated because of the interaction of P−OH groups with NH_3 molecules, which can shift the P−OH band toward a lower wavenumber.[45−47] This observation suggests the accessibility of P−OH acidic groups to NH_3 molecules. It is well-known that the extent of the shift can be used to evaluate the acidity of hydroxyl groups. A shift value of around 420 cm^{-1} is obtained and is smaller than that of the silanols present in zeolites.[46,47] This evidences the relatively weak acidity of our present hierarchically porous $TiPO_4$ materials. Another band at around 1430 cm^{-1}, corresponding to the surface-adsorbed NH_4^+ groups, emerges (Figure 13c). Despite the weak acidity of P−OH groups, they are acid enough to interact with NH_3 molecules to form NH_4^+ ions.[46,47] The desorption was then performed at different temperatures. The intensity of the band at 3670 cm^{-1} is progressively recovered, and the band intensity at 1430 cm^{-1} decreases with the increase in the desorption temperature (Figure 14d−f), indicating that the ammonia adsorption and desorption processes are reversible, and that the weakly acidic P−OH groups regenerate upon the increase in desorption temperature, as observed in the case of acidic zeolites.

Discussion. SEM, TEM, and N_2 adsorption analysis evidence the successful synthesis of the first bimodal hierarchically macroporous TiPO materials with mesoporous walls by a template-free spontaneous formation mechanism.[26,27,29] The macrochannels with diameters of 50−160 nm in these TiPO materials are not well arranged, and their number is not as abundant (Figure 1) as that in other pure metal oxides with similar hierarchical structure. Metal alkoxides are essential for the formation of meso-macroporous structures because of the high hydrolysis and polycondensation rates. The generation of hierarchically meso-macroporous structures is a self-formation phenomenon. A large series of other titanium chemical precursors have been examined, and no such structure can be obtained, showing the importance of an inorganic precursor. The addition of a small content (5 wt %) of a neutral surfactant can not only help to expand the macropore size to 80−250 nm (Figure 2), but it can also generate abundant and well-arranged macrochannels. Interestingly, the second largest macroporosity can be introduced in the hierarchical bimodal meso-macroporous structure, leading to the triple porous system integrated into one solid body when the surfactant content is raised to 10 wt % in the reaction system. Further increasing the surfactant content to 15 wt % results in the formation of a three-dimensional (3D) co-continuous macroporous structure with an enlarged macropore-size. This suggests that surfactant may play a supplementary but no direct role in the formation of hierarchical porosity. The previously reported macroporous titanias synthesized template-free in basic conditions had very large channel diameters of micrometer scale.[26] Comparatively, the present TiP−N sample has a uniform submicrometer-sized small macropore array with mesoporous walls. The macroporosity could be improved by the addition of surfactant (such as the sample TiP−S5). The TiP−S10 has bimodal macropores of mesoporous frameworks, and the TiP−S15 has a co-continuous macroporous structure, all of which have never been reported before, and should be of great significance from a technological point of view. Although the hierarchically meso-macroporous structures can be generated either by a spontaneous process or by a soft templating method, neither one allows control of macropore size or induces trimodal porosity (one mesoporosity and two macroporosity) in one solid body. The present work is a clear demonstration of tailoring the porous hierarchy of materials by fine-tuning the self-formation process and the participation of a neutral surfactant.

The hierarchical mesoporous−macroporous structure of TiP−N is spontaneously formed because no templatable agents are added in the synthesis. The hydrolysis of Ti−alkoxide precursors in the phosphate solution would result in the formation of nanometer-sized TiPO particles. A lot of propanol molecules were quickly and simultaneously generated by the reaction of $Ti(PrO)_4$ and phosphatic ions and polycondensation, which might produce microphase-separated domains of TiPO-based nanoparticles and water/alcohol channels,[26,27,48] initiating the production of macroporous structures. The regular self-assembly of the nanoparticles will create a well-connected network of narrow mesoporous channels. Thus, a hierarchical structure of uniform macrochannels with mesoporous walls of nanoparticle assembly would self-form during the synergistic packing of the nanoparticles.

A small quantity of surfactant molecules added in the reaction system would interact with propanol molecules to form organic-rich phases with larger domains, leading to the production of improved macroporosity. Large macropores are only present in the TiP−S*x* samples synthesized at high surfactant contents (i.e., ≥ 10 wt % in the present work). This is due to the excess surfactants aggregating on the surface of TiPO nanoparticles, followed by the phase separation of inorganic-rich and surfactant-rich mesophases during aging.[49] The bimodal macroporous structure of surfactant-synthesized TiPO should be the result of the presence of two kinds of organic-rich phases (i.e., one originated from alcohol by-products (or the mixture of alcohol and surfactant) and another originated from surfactant). It is reasonable that the increase in surfactant content would modify the property of the surfactant-rich phases, and thus a 3D co-continuous macroporous TiPO would be fabricated thereof in the presence of a very high content of surfactant molecules (e.g., 15%).

Previous studies have suggested the relationship between surfactant molecules and the resultant macroporosity.[17,21] Our current work also further presents that the macroporous structure could be tunable by a variation in surfactant concentration. In comparison with the TiPOs synthesized with and without surfactant, there is no significant improvement in the surface area, pore volume, and local orderliness of the mesopores in the networks of all hierarchical TiPOs for the surfactant-assisted synthesis. Although the surfactant may play a small role in inducing the regular organization of mesopores formed by nanoparticle assembly, the aggregation of nanoparticles can be influenced by surfactant molecules because of the interaction between the nanoparticles of TiPO−surfactant. That is why, in our study, we observed a change in mesoporosity (pore homogeneity and pore size; Figures 6 and 7) with the addition of surfactant. However, the phenomenon of the interaction of

(45) Su, B. L.; Barthomeuf, D. *J. Catal.* **1993**, *139*, 81−92.
(46) Su, B. L.; Norberg, V.; Hansenne, C. *Langmuir* **2000**, *16*, 1132−1140.
(47) Su, B. L.; Norberg, V. *Colloids Surf., A.* **2001**, *187−188*, 281−286.
(48) Ren, T. Z.; Yuan, Z. Y.; Su, B. L. *Chem. Phys. Lett.* **2004**, *388*, 46−49.
(49) Vrieling, E. G.; Beelen, T. P. M.; van Santen, R. A.; Gieskes, W. W. C. *Angew. Chem., Int. Ed.* **2002**, *41*, 1543−1546.

surfactant molecules with inorganic species is not totally understood since it is not clear yet whether the formation of mesostructured phases is based on the interaction of a single surfactant with inorganic species or on the interaction between the aggregates of surfactants with inorganic species. Because of our experience and the present work, an intimate interaction between surfactants and inorganic species could occur.

The present meso-macroporous TiPOs are thermally stable after calcination at 550 °C despite their amorphous nature. FT-IR, XPS, and NMR spectra confirmed the presence of a Ti−O−P network with Ti/P ratios of ∼1. No discrete phases (such as titanium oxyphosphate, polyphosphate, and anatase) were observed in the samples after calcination. It is also revealed that a large quantity of acidic surface hydroxyl groups (including P−OH) existed in these hierarchical TiPOs, and the proton conductivity and ion-exchange capacity are expected. The optical property is also investigated. It is thus believed that, because of their attractive properties, such hierarchical TiPO materials could be significant and find numerous practical applications from catalysis and separation to electrochromic devices, fuel cells, and supercapacitors, as well as bioactive materials. The hierarchical porous structures of these TiPO materials are similar to those observed in bone tissues. It is mentioned that, in bone implant, the binding between Ti metal and calcium phosphate is difficult. The titanium phosphate materials reported here might be an interesting alternative candidate as bone substitute for bone tissue engineering.

Conclusions

The integration of multiscaled and tunable porosity leading to the formation of hierarchically mesoporous−macroporous titanium phosphate materials has been demonstrated by adjusting the template-free self-formation phenomenon and the participation of a neutral surfactant. The macroporosity could be tunable by the content of the surfactant added. First, well-defined, small, macroporous structures of TiPO were spontaneously produced in the absence of any templatable agents, including surfactant molecules. The high hydrolysis and polycondensation rates of metal alkoxides with rapid liberation of a huge amount of alcohol molecules could be the source of the self-generation of macrochannels. On this basis, the macropore sizes could then be enlarged from 50−160 to 80−250 nm by the addition of a small quantity of nonionic poly(ethylene oxide) surfactant (e.g., 5 wt %), accompanying the improvement of the macroporosity in abundance and in regularity. A secondary large-macropore system with parallel channels that are 500−1000 nm in size was obtained in the presence of 10 wt % of surfactant, leading to the bimodal macroporous structure. Further increasing the surfactant content to 15 wt % resulted in the formation of a uniform 3D co-continuous macroporous structure. All the walls between the macropores of these TiPO materials are composed of accessible mesopores with a wormhole-like array, followed by the nanoparticle assembly mechanism. Although the surfactant molecules did not play an important role during the formation of macroporosity, they can influence the mesoporosity formed by the assembly of nanoparticles[28] and can be used to tune the macroporosity and to create supplementary macroporosity on the basis of the self-formation process. The frameworks of these synthesized hierarchical TiPO materials are amorphous with Ti−O−P bonding, exhibiting high thermal stability according to the XRD, XPS analysis, FT-IR, and NMR spectra. The optical and acidic properties are present in these hierarchical TiPO materials. The interesting concept developed in this work could be extended toward the controlled assembly of a variety of materials by controlling the balance between seed crystal formation, growth, and aggregation. Undoubtedly, this occurs in many other systems as well, although it may be unappreciated. We are convinced that the present work contributes to the fundamental science of surfactant-mediated porous materials development, which could lead to guidelines to make tailored materials. However, at the moment, the mesoporous system formed by the assembly of nanoparticles still remains a disordered framework with wormhole-like channels, even though there are surfactant molecules in the synthesis media. Improving organization and tuning the mesopore size as desired is therefore still a great experimental challenge.[50−53] Other surfactant molecules such as triblock copolymers and neutral alkylamines have to be used to check whether these surfactant molecules can lead to better organization of the mesoporous framework as well as the macroporous architectures and tune the pore sizes and the hierarchy of both systems. Our very recent work already made significant advances in the formation of hierarchical materials. It is also interesting to extend this expertise in the synthesis of titanium phosphates to other compositions, since many potential applications are reasonably expected for these hierarchical meso-macroporous structures.

Acknowledgment. This work was supported by the European Program of InterReg III (Programme France-Wallonie-Flandre, FW-2.1.5), the Belgian Federal Government PAI-IUAP 01/5 project, the Région Wallonne, Belgium, the National Natural Science Foundation of China (No. 20473041), and the National Basic Research Program of China (No. 2003CB615801).

LA0533011

(50) Yuan, Z. Y.; Ren, T. Z.; Azioune, A.; Pireaux, J. J.; Su, B. L. *Catal. Today* **2005**, *105*, 647−654.
(51) Yuan, Z. Y.; Ren, T. Z.; Azioune, A.; Pireaux, J. J.; Su, B. L. *Chem. Mater.* **2006**, *18*, doi10.1021.
(52) Yuan, Z. Y.; Su, B. L. *J. Chem. Mater.* **2006**, *16*, 663−677.
(53) Vantomme, A.; Yuan, Z. Y.; Su, B. L. *New J. Chem.* **2004**, *28*, 1083−1085.